

Possibilistic approach to network nonlocality

Antoine Restivo^{1,2}, Nicolas Brunner¹, and Denis Rosset¹

¹Department of Applied Physics University of Geneva, 1211 Geneva, Switzerland

²Centre for Quantum Information and Communication, École polytechnique de Bruxelles, Université libre de Bruxelles, CP 165, 1050 Brussels, Belgium

The investigation of Bell nonlocality traditionally relies on joint probabilities of observing certain measurement outcomes. In this work we explore a possibilistic approach, where only patterns of possible outcomes matter, and apply it to Bell nonlocality in networks with independent sources. We present various algorithms for determining whether a given outcome pattern can be achieved via classical resources or via non-signaling resources. Next we illustrate these methods considering the triangle and square networks (with binary outputs and no inputs), identifying patterns that are incompatible with the network structure, as well as patterns that imply nonlocality. In particular, we obtain an example of quantum nonlocality in the square network with binary outcomes. Moreover, we show how to construct certificates for detecting the nonlocality of a certain pattern, in the form of nonlinear Bell-type inequalities involving joint probabilities. Finally, we show that these inequalities remain valid in the case where the sources in the network become partially correlated.

1 Introduction

Recently, growing interest has been devoted to the question of quantum nonlocality in networks. From a fundamental perspective, this new area of research aims at characterizing quantum correlations in a network configuration, where several independent sources distribute entangled states to subsets of nodes (parties). From a more practical point of view, these ideas are also connected to the development of future quantum communication networks.

This area of research already brought significant contributions; see e.g. [1] for a recent review. The key idea is to characterize correlations in networks under the assumption that the different sources are independent from each other [2]. Notably, it was shown that the network configuration allows for novel forms of quantum nonlocal correlations, departing radically from standard quantum Bell nonlocality. The first striking example is the fact that quantum nonlocality can be demonstrated without the needs of different measurement settings (i.e. each party performs a sin-

gle fixed measurement) [3, 4]. This effect is known as “quantum nonlocality without inputs”, of which more examples have been reported [5, 6, 7, 8, 9, 10]. Moreover, the use of non-classical measurements (such as the well-known Bell-state measurement) allows for quantum nonlocal correlations that are genuine to the network structure [11, 12].

More generally, it is fair to say that a general understanding of nonlocality in networks is still far away. Among the main challenges is the characterisation of local correlations in a given network structure (i.e. characterize those probability distributions that admit a classical model), which turns out to be extremely challenging. All methods developed in the context of (standard) Bell nonlocality are mostly useless here, and novel methods must be developed, see e.g. [2, 13, 14, 15, 16, 17, 18, 19, 20]. The main difficulty arises from the independence assumption of the various sources in the network, which makes the problem nonlinear and highly nontrivial. Another challenging problem is to characterize the limits on correlations imposed by the no-signaling principle [21, 15, 22]. Both of these questions are fundamental towards a better understanding of quantum nonlocality in networks.

In the present work, we explore a possibilistic approach to the question of nonlocality in networks. This approach provided deep insight in the context of standard Bell nonlocality (most notably through the well-known Hardy [23] and Greenberger-Horne-Zeilinger [24, 25] paradoxes). The possibilistic approach in the context of networks has been proposed by Wolfe, Spekkens and Fritz [15], and Fraser [26] developed an efficient algorithm for the case of local models, but no systematic investigation has been reported so far. As we will see, this offers a new perspective on the problem of characterizing local, quantum and no-signaling correlations in networks.

The main idea is to move away from probabilities, and consider only possibilities. That is, we are only interested to know if an event (e.g. a certain combination of measurement outputs) occurs with some non-zero probability or, on the contrary, is impossible (i.e. has probability zero). We then ask which patterns (i.e. a combination of possible and impossible events) are compatible with a local, quantum and non-signaling model for a given network struc-

ture. We present several methods to attack this question, relying on the inflation technique, SAT solvers and efficient combinatorial algorithms. Next we apply it to specific examples, namely the well-known “triangle network” and the square network (both for the case of binary outputs and without inputs) and classify all patterns. Moreover, our methods allow for the derivation of non-linear Bell-type inequalities for networks, which can then be applied to actual probability distributions. We use these inequalities to show that any pattern that is incompatible with a local model (assuming fully independent sources) is also incompatible with a local model where the different sources can be partially correlated [27].

We start in Section 2 by describing the generalized Bell scenarios in which we operate, and define not only the probability distributions that are observed, but also the possibilistic patterns and their symmetries. We mention the triangle and square scenarios, whose orbits we classify in this paper. We describe the different sets of correlations (local, quantum and non-signaling) and list the algorithms that can be used to test for membership. In Section 3 we describe the algorithms to decide whether a pattern or probability distribution is non-signaling. We define formally the inflations of a given scenario and the possibilistic approach to the inflation technique. In Section 4 we do the same for the set of network-local correlations. We then present in Sections 5 and 6 the classification results for the triangle and square scenarios, respectively. We also present an instance of quantum nonlocality in the square network with binary outcomes. Finally, in Section 7, we show that we can derive inequalities robust under a relaxation of the source independence assumption.

2 Generalized Bell-like scenarios

We consider a generalized Bell-like scenario containing sources and observers, where the sources distribute information of classical, quantum or post-quantum nature to the observers. In turn, each observer processes this information to provide a classical outcome taken from a finite set of values; for simplicity we restrict observers to a single fixed measurement. This leads to the formal definition below.

Definition 1. A scenario \mathbb{S} is described by a directed bipartite graph $\mathbb{S} = (\mathcal{S}, \mathcal{O}, \mathcal{E})$, where a set of sources $\mathcal{S} = \{\mathcal{S}_i\}_{i \in \mathcal{I}}$ and a set of observers $\mathcal{O} = \{\mathcal{O}_j\}_{j \in \mathcal{J}}$ are connected by directed edges $\mathcal{E} \subseteq \{(\mathcal{S}_i, \mathcal{O}_j) : i \in \mathcal{I}, j \in \mathcal{J}\}$, with the index sets $\mathcal{I} = \{1, \dots, |\mathcal{I}|\}$ and $\mathcal{J} = \{1, \dots, |\mathcal{J}|\}$. Each observer \mathcal{O}_j produces an outcome $o_j \in \{1, \dots, n_j\}$, and we include in \mathbb{S} the number of outcome values $\{n_j\}$ as a label on the observer vertices \mathcal{O} .

We observe the correlations in this scenario and describe them using a probability distribution

$P_{\{\mathcal{O}_j\}_{j \in \mathcal{J}}}(o_1, \dots, o_{|\mathcal{J}|})$. The coefficients in P are non-negative and obey the normalization constraint:

$$\sum_{o_1, \dots, o_{|\mathcal{J}|}} P(o_1, \dots, o_{|\mathcal{J}|}) = 1. \quad (1)$$

Without loss of generality, we assume that each observer is connected to at least one source, otherwise the probability distribution can be factorized to leave those observers out of the questions we tackle.

Geometrically speaking, we can enumerate the coefficients of $P_{\{\mathcal{O}_j\}_{j \in \mathcal{J}}}$ into a vector $\vec{P}_{\mathcal{J}} \in \mathbb{R}^{n_1 \dots n_{|\mathcal{J}|}}$; in this paper we chose to increment the outcome of the last observer first. Accordingly, we enumerate the vectors of the Euclidean basis as $\{\vec{e}_{o_1 \dots o_{|\mathcal{J}|}}\}_{o_1 \dots o_{|\mathcal{J}|}}$.

Definition 2. The elements of the Euclidean basis of the vector space of probability distributions are written:

$$[o_1 \dots o_{|\mathcal{J}|}] \equiv \vec{e}_{o_1 \dots o_{|\mathcal{J}|}} \quad (2)$$

We thus have:

$$\vec{P} = \sum_{o_1 \dots o_{|\mathcal{J}|}} P(o_1 \dots o_{|\mathcal{J}|}) \cdot [o_1 \dots o_{|\mathcal{J}|}] \quad (3)$$

Definition 3. Let $\mathcal{K} \subseteq \mathcal{J}$ be indices that describe a subset of observers. We write $P_{\{\mathcal{O}_j\}_{j \in \mathcal{K}}}$ the corresponding marginal probability distribution and likewise the probability vector $\vec{P}_{\mathcal{K}}$.

This vector can be computed according to

$$\vec{P}_{\mathcal{K}} = M_{\mathcal{K}, \mathcal{J}} \cdot \vec{P}_{\mathcal{J}} \quad (4)$$

where $M_{\mathcal{K}, \mathcal{J}}$ is a matrix with 0/1 entries that represents the marginalization step. Probability distributions are described with nonnegative real coefficients; marginalization and most operations used in this paper only involve addition and multiplication. Thus the relevant algebraic structure is the commutative semiring $(\mathbb{R}^{\geq 0}, +, \cdot)$ where $\mathbb{R}^{\geq 0} = [0, \infty[$.

2.1 Possibilities and patterns

We can obtain good insights about a given scenario by considering *possibilities* instead of probabilities.

Definition 4. A possibility $\mathfrak{p} \in \{\circ, \checkmark\} = \mathbb{P}$ is a binary value where \circ designates that a given event will never occur, while \checkmark designates that it can happen with non-zero probability.

Moving to a possibilistic picture is of great interest since for a given number of parties, the associated set of patterns is finite. Indeed, for n observers with m possible outcomes, one can define m^n possible patterns. Hence, it is possible to sort them completely. As we will see, one can directly map the operations on possibilities to binary Boolean algebra. This peculiarity allows us to formulate the marginal compatibility

problem into a Boolean satisfiability problem, which is easier to solve than linear programs.

For two disjoint events with possibilities \mathbf{p}_1 and \mathbf{p}_2 , we can compute the possibility of either or both of them happening as $\mathbf{p}_1 + \mathbf{p}_2$ with

$$\circ + \circ = \circ, \quad \circ + \checkmark = \checkmark + \circ = \checkmark + \checkmark = \checkmark. \quad (5)$$

Considering now two uncorrelated events with possibilities \mathbf{p}_1 and \mathbf{p}_2 , the possibility for both to occur $\mathbf{p}_1 \cdot \mathbf{p}_2$ is given by

$$\circ \cdot \circ = \circ \cdot \checkmark = \checkmark \cdot \circ = \circ, \quad \checkmark \cdot \checkmark = \checkmark. \quad (6)$$

The set $\mathbb{P} = \{\circ, \checkmark\}$, equipped with addition $+$ and the multiplication \cdot described above is a commutative semiring $(\mathbb{P}, +, \cdot)$. The semiring is ordered ($\circ < \checkmark$), and this order is compatible with addition.

Given a probability $P \in \mathbb{R}^{\geq 0}$, the corresponding possibility \mathbf{p} is

$$\mathbf{p} = \begin{cases} \circ, & P = 0, \\ \checkmark, & P > 0. \end{cases} \quad (7)$$

The latter transformation defines a morphism $\varphi : \mathbb{R}^{\geq 0} \rightarrow \mathbb{P}$, and it is easy to verify that this morphism preserves the semiring structure ($\varphi(x + y) = \varphi(x) + \varphi(y)$, $\varphi(x \cdot y) = \varphi(x) \cdot \varphi(y)$) and the ordering ($x \leq y \Rightarrow \varphi(x) \leq \varphi(y)$). Using this morphism, we can translate statements about probabilities into statements about possibilities.

Two particular transformations are interesting. Let $x, y, z \in \mathbb{P}$. Then:

$$x + y + z = \circ \quad \Rightarrow \quad x = y = z = \circ, \quad (8)$$

$$x + y + z = \checkmark \quad \Rightarrow \quad (x = \checkmark) \vee (y = \checkmark) \vee (z = \checkmark). \quad (9)$$

From the probability distribution $\vec{P}_{\mathcal{J}} \in \mathbb{R}^N$, we compute the *pattern* $\vec{\mathbf{P}}_{\mathcal{J}} \in \mathbb{P}^N$ using the morphism $\vec{\mathbf{P}}_{\mathcal{J}} = \varphi(\vec{P}_{\mathcal{J}})$. Each pattern $\vec{\mathbf{P}}_{\mathcal{J}}$ corresponds to many distributions $\vec{P}_{\mathcal{J}}$, and we call the set of those preimages

$$\varphi^{-1}(\vec{\mathbf{P}}_{\mathcal{J}}) \subset \mathbb{R}^N \quad (10)$$

the *realizations* of the pattern $\vec{\mathbf{P}}_{\mathcal{J}}$.

We note that not all patterns are physical. Using the morphism φ , we rewrite (1) into a possibilistic statement

$$\sum_{o_1, \dots, o_{|\mathcal{J}|}} P(o_1, \dots, o_{|\mathcal{J}|}) = \checkmark \quad (11)$$

which is not satisfied by the pattern $\vec{\mathbf{P}}_{\mathcal{J}} = (\circ, \circ, \dots, \circ)$.

In a given scenario, the number of patterns satisfying the normalization condition is $2^{o_1 \dots o_{|\mathcal{J}|}} - 1$.

2.2 Symmetries

We work within the device-independent framework, and thus the labeling of sources, observers and outcomes has no specific meaning. We consider in turn relabelings of outcomes and relabelings of sources/observers.

We first consider the relabeling of outcomes. For a given j , consider the classical outcome $o_j \in \{1, \dots, |n_j|\}$. We can permute those labels with a permutation $\pi_j \in S_{n_j}$ without changing the underlying physics, with S_{n_j} is the symmetric group of degree n_j .

Definition 5. *The group of outcome relabelings G_{outcomes} is the direct product $G_{\text{outcomes}} = S_{n_1} \times \dots \times S_{n_{|\mathcal{J}|}}$. Its elements are written $\pi = (\pi_1, \dots, \pi_{|\mathcal{J}|}) \in G_{\text{outcomes}}$.*

Consider $\pi \in G_{\text{outcomes}}$ and a probability distribution \vec{P} , we write using (3):

$$\pi(\vec{P}) = \sum_{o_1 \dots o_{|\mathcal{J}|}} P(o_1 \dots o_{|\mathcal{J}|}) \cdot [\pi_1(o_1), \dots, \pi_{|\mathcal{J}|}(o_{|\mathcal{J}|})]. \quad (12)$$

We now consider relabelings of sources and observers.

Definition 6. *The group of observers relabelings $G_{\text{observers}}$ is derived from the automorphism group of the directed bipartite graph \mathbb{S} , by considering its action on observers: $G_{\text{observers}} \subset S_{|\mathcal{J}|}$.*

We write the action of $\sigma \in G_{\text{observers}}$ on a probability distribution:

$$\sigma(\vec{P}) = \sum_{o_1 \dots o_{|\mathcal{J}|}} P(o_1 \dots o_{|\mathcal{J}|}) \cdot [o_{\sigma^{-1}(1)} \dots o_{\sigma^{-1}(|\mathcal{J}|)}]. \quad (13)$$

Definition 7. *A relabeling $g = (\sigma, \pi)$ in the scenario \mathbb{S} is composed of a member of $G_{\text{observers}}$ and G_{outcomes} . The relabeling group $G = G_{\text{observers}} \times G_{\text{outcomes}}$ is a semidirect product constructed using the natural action of $G_{\text{observers}}$ on the elements of G_{outcomes} .*

A relabeling $g \in G$ acts on probability distributions as $g(\vec{P}) = (\sigma, \pi)(\vec{P}) = \sigma(\pi(\vec{P}))$. However, all we care about in this paper is the enumeration of relabelings in G , and the exact structure of G is not relevant for that purpose.

Relabelings of probability distributions translate into relabelings of patterns. The group G is especially interesting when studying all possible patterns of a scenario, as to group them.

Definition 8. *Under the action of G , a pattern $\vec{\mathbf{P}}$ correspond to an orbit $\vec{\mathbf{P}}^G$ of patterns with similar physical properties:*

$$\vec{\mathbf{P}}^G = \{g(\vec{\mathbf{P}}) : g \in G\}. \quad (14)$$

As an example, the nonphysical pattern $(\circ, \circ, \dots, \circ)$ is the only member of its orbit.

To make the definitions above concrete, we turn to the two scenarios considered in this paper.

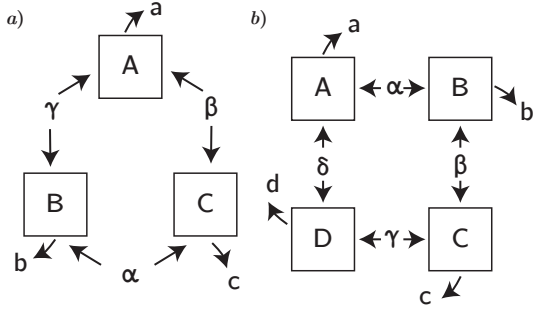


Figure 1: Scenarios considered in this paper: a) the triangle scenario, b) the square scenario

2.3 The triangle scenario

The triangle scenario involves three sources $\mathcal{S} = \{\alpha, \beta, \gamma\}$ and three observers $\mathcal{O} = \{A, B, C\}$, with connections $\mathcal{E} = \{(\alpha, B), (\alpha, C), (\beta, A), (\beta, C), (\gamma, A), (\gamma, B)\}$, as shown in Figure 1a. We consider binary outcomes $a, b, c \in \{0, 1\}$. A probability distribution $\vec{P}_{ABC} \in \mathbb{R}^8$ in this scenario has the coefficients:

$$\vec{P}_{ABC} = (P(000), P(001), P(010), P(011), \dots, P(100), P(101), P(110), P(111))^\top. \quad (15)$$

The symmetry group G_{outcomes} has 8 elements, and the automorphism group $G_{\text{observers}}$ is the symmetry group of the triangle, i.e. the dihedral group of order 6: $D_6 = S_3$.

This scenario contains $255 = 2^{2 \cdot 2 \cdot 2} - 1$ patterns satisfying normalization. Using relabelings, they are grouped into 21 orbits.

2.4 The square scenario

The square scenario involves four sources $\mathcal{S} = \{\alpha, \beta, \gamma, \delta\}$ and four observers $\mathcal{O} = \{A, B, C, D\}$, with connections

$$\mathcal{E} = \{(\alpha, A), (\alpha, B), (\beta, B), (\beta, C), (\gamma, C), (\gamma, D), (\delta, D), (\delta, A)\}, \quad (16)$$

as shown in Figure 1b. Again we consider binary outcomes $a, b, c, d \in \{0, 1\}$. We write a probability distribution $\vec{P}_{ABCD} \in \mathbb{R}^{16}$. The symmetry group G_{outcomes} has 16 elements, and the automorphism group $G_{\text{observers}}$ is the symmetry group of the square, i.e. the dihedral group of order 8, namely D_8 .

The scenario contains $65535 = 2^{2 \cdot 2 \cdot 2 \cdot 2} - 1$ patterns satisfying normalization. Under relabelings, they are grouped into 804 orbits.

2.5 Correlation sets and decision problems

Depending on the type of resources that the sources $\{\mathcal{S}_i\}$ distribute, we may observe different sets of correlations. Among the sets of interest, we distinguish three.

Definition 9. The nonsignaling set $\mathcal{N} \subset \mathbb{R}^N$, containing probability distributions that do not enable signaling.

Definition 10. The quantum set $\mathcal{Q} \subseteq \mathcal{N} \subset \mathbb{R}^N$, containing probability distributions obtained when the sources distribute quantum states which are measured by the observers according to the axioms of quantum mechanics.

Definition 11. The local set $\mathcal{L} \subseteq \mathcal{Q} \subseteq \mathcal{N} \subset \mathbb{R}^N$, containing probability distribution obtained by processing classical information. There we identify sources with local hidden variables, and the processing follows from classical probability axioms.

For each of these sets, we aim to answer the decision problem: is $\vec{P} \in \mathcal{N}, \mathcal{Q}, \mathcal{L}$? When the answer is, e.g., $\vec{P} \in \mathcal{L}$, we may want a *model* that shows explicitly how, e.g., \vec{P} can be obtained using local hidden variables. When the answer is negative (e.g., $\vec{P} \notin \mathcal{L}$), we may want a *certificate*, i.e. a statement of non-membership that is nevertheless easier to verify than solving the decision problem once again.

As the labeling of sources, observers and outcomes is arbitrary, for a given relabeling $g \in G$, we have

$$g(\vec{P}) \in \mathcal{N} \Leftrightarrow \vec{P} \in \mathcal{N}, \quad (17)$$

and the same for the sets \mathcal{Q} and \mathcal{L} .

As we discuss in the next sections, those decision problems are hard and scale badly with the number of sources, observers and outcomes. Solving those problems on patterns can be much easier. We write $\mathbb{N}, \mathbb{Q}, \mathbb{L}$ for the sets of patterns corresponding to $\mathcal{N}, \mathcal{Q}, \mathcal{L}$: the pattern $\vec{P} \in \mathbb{N}$ if there exists $\vec{P} \in \mathcal{N}$, and so on.

As the number of all patterns for a given scenario is finite, we can group them according to the layers shown in Figure 2. The techniques and algorithms are described in Table 1.

2.6 Certificates

We now turn to certificates. They describe in a compact manner that a set of distributions or patterns is *not* in a correlation set. In our paper, they are the result of an algorithm solving a decision problem, and subsequently testing the validity of a certificate is easier than solving the decision problem in the first place.

Definition 12. Following [15], a valuation V is an assignment of outcomes to a subset of parties of a scenario.

For example, in the triangle scenario $\{a = 0, c = 1\}$ is a valuation on the observers A and C. It corresponds to the probability $P(V) = P_{AC}(01)$. For a given scenario \mathbb{S} , we consider the set \mathbf{V} of all valuations. Let $V_1, \dots, V_m \in \mathbf{V}$ be arbitrary valuations.

Decision problem	Exact algorithm	Relaxation: find a model	Relaxation: find imp. certificate
$\vec{P}_{\text{test}} \in \mathcal{N}$?	?	Alg. 1
$\vec{P}_{\text{test}} \in \mathcal{N}$?	?	Alg. 2 and 3
$\vec{P}_{\text{test}} \in \mathcal{Q}$?	Nonconvex optimization [28]	Inflation&SDP [29, 30]
$\vec{P}_{\text{test}} \in \mathcal{Q}$?	?	?
$\vec{P}_{\text{test}} \in \mathcal{L}$	Alg. 5	Same as left, red. cardinality	Alg. 7
$\vec{P}_{\text{test}} \in \mathcal{L}$	Alg. 6, Alg. 9	Same as left, red. cardinality	Alg. 8

Table 1: Decision problems and available techniques

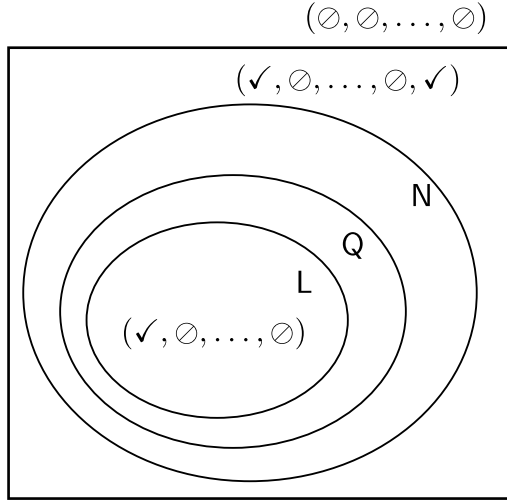


Figure 2: Local (L), quantum (Q) and nonsignaling (N) sets of patterns, with examples of patterns in the triangle scenario. The rectangle contains only patterns that satisfy the normalization condition. In the triangle scenario, the pattern $[000]$ is obviously local, and the pattern $[000] + [111] \notin \mathcal{N}$.

Definition 13. A monomial $M = P(V_1) \dots P(V_m)$ of degree $\deg M = m$ is defined by a sequence (V_1, \dots, V_m) of m valuations. For a given scenario \mathbb{S} , we write \mathbf{M} the set of all its monomials.

For example, the monomial $P_{ABC}(000)$ has degree 1 while $P_A(0)P_B(0)$ has degree 2.

Definition 14. A certificate I for the correlation set $\mathcal{X} \in \{\mathcal{L}, \mathcal{Q}, \mathcal{N}\}$ is a polynomial $I \in \mathbb{R}\mathbf{M}$ (a formal sum over \mathbf{M}) with the condition that

$$\vec{P} \in \mathcal{X} \Rightarrow I(\vec{P}) \geq 0. \quad (18)$$

The degree of a polynomial $I \in \mathbb{R}\mathbf{M}$ is given by the maximal degree of all its monomials.

3 Nonsignaling correlations

In (1) and in (11), we asserted that correlations must obey the normalization constraint. However, there are other constraints that come into play. We start with an example.

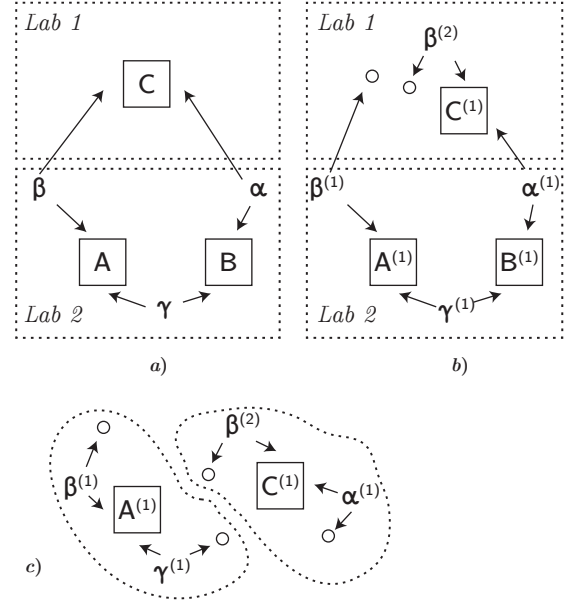


Figure 3: Construction of nonsignaling condition: a) the original triangle scenario, b) a variant of the scenario involving a copy of the source γ , c) a variant of the scenario involving a copy of the source γ and removing B .

3.1 Nonsignaling constraints

Let us look at the triangle scenario in Figure 3a. In Figure 3b, we construct a variant of the scenario by duplicating the source β ; we also added indices to sources and observers to distinguish them from the original scenario.

In both scenarios, if we examine the probability distributions \vec{P}_{AB} and $\vec{P}_{A^{(1)}B^{(1)}}$, these distributions must be identical due to the no signaling principle, as the devices present in the second lab are identical. Indeed, if $\vec{P}_{AB} \neq \vec{P}_{A^{(1)}B^{(1)}}$, then the first lab could signal to the second lab by changing the wiring. We thus have $\vec{P}_{AB} = \vec{P}_{A^{(1)}B^{(1)}}$. By changing the lab boundaries, we also get $\vec{P}_{BC} = \vec{P}_{B^{(1)}C^{(1)}}$. Finally, we observe that removing $B^{(1)}$ leads to the scenario in Figure 3c, where we must have $P_{A^{(1)}C^{(1)}}(ac) = P_{A^{(1)}}(a)P_{C^{(1)}}(c)$.

We now consider the pattern $\vec{P}_{ABC}^{\text{GHZ}} = [000] + [111] = (\checkmark, \circ, \circ, \circ, \circ, \circ, \circ, \checkmark)^\top$, slightly abusing the notation (2). If that pattern obeys the nonsignaling principle, there must be a pattern $\vec{P}_{A^{(1)}B^{(1)}C^{(1)}}$ such

that

$$\begin{aligned}\vec{P}_{A^{(1)}B^{(1)}} &= \vec{P}_{AB}, \\ \vec{P}_{B^{(1)}C^{(1)}} &= \vec{P}_{BC}, \\ P_{A^{(1)}C^{(1)}}(ac) &= P_A(a)P_C(c).\end{aligned}\quad (19)$$

We have thus:

$$\vec{P}_{A^{(1)}B^{(1)}} = \vec{P}_{B^{(1)}C^{(1)}} = (\checkmark, \emptyset, \emptyset, \checkmark). \quad (20)$$

We also have $P_A(a) = P_C(c) = \checkmark$ and thus:

$$\vec{P}_{A^{(1)}C^{(1)}} = (\checkmark, \checkmark, \checkmark, \checkmark) \quad (21)$$

Using the statements (8) and (9), we have:

a	b	c	$P_{A_1B_1C_1}$ of (20)	$P_{A_1B_1C_1}$ of (21)
0	0	0	\checkmark	
0	0	1	\emptyset	χ_1
0	1	0	\emptyset	
0	1	1	\emptyset	χ_2
1	0	0	\emptyset	ω_1
1	0	1	\emptyset	
1	1	0	\emptyset	ω_2
1	1	1	\checkmark	

where $(\chi_1 = \checkmark) \vee (\chi_2 = \checkmark)$ and $(\omega_1 = \checkmark) \vee (\omega_2 = \checkmark)$, which leads to a contradiction.

We say that the pattern $\vec{P}_{ABC}^{\text{GHZ}} = [000] + [111]$ is *signaling-enabling*; if we had a scenario with those correlations, the modification of this scenario as in Figure 3b would enable signaling. This statement means that all realizations of $\vec{P}_{ABC}^{\text{GHZ}}$ in the sense of (10), written

$$\vec{P}_{ABC}^{\text{GHZ}} = (x, 0, 0, 0, 0, 0, 0, 1-x), \quad (22)$$

are also signaling-enabling for $0 < x < 1$. Finally, we note that the orbit of $\vec{P}_{ABC}^{\text{GHZ}}$ is also *signaling-enabling*:

$$(\vec{P}_{ABC}^{\text{GHZ}})^G = \{[000] + [111], [001] + [110], [010] + [101], [011] + [100]\}. \quad (23)$$

3.2 Inflations and nonsignaling inflations

In the Figure 3 we used in the previous section, we presented an example of a modification of the original scenario. Such a modification is called an *inflation*, following the process proposed by [15].

Definition 15. An inflation contains copies of the original sources and observers, wiring them according to the template of the original scenario. In the inflation $\mathcal{S}' = (\mathcal{S}', \mathcal{O}', \mathcal{E}')$, we write with $\mathcal{S}' = \{\mathcal{S}_i^{(k)}\}$ and $\mathcal{O}' = \{\mathcal{O}_j^{(l)}\}$. We wire them according to the following rules.

- *Compatible types:*

$$(\mathcal{S}_i^{(k)}, \mathcal{O}_j^{(l)}) \in \mathcal{E}' \Rightarrow (\mathcal{S}_i, \mathcal{O}_j) \in \mathcal{E}, \quad (24)$$

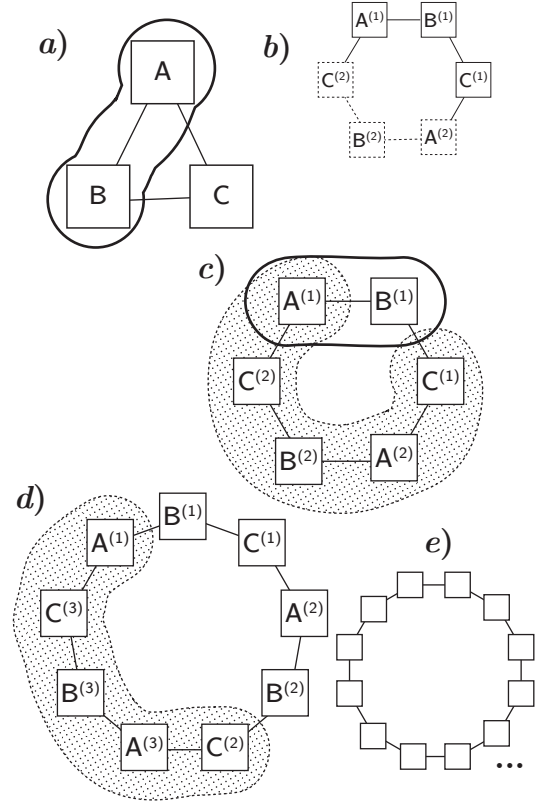


Figure 4: Complete family of inflations for the triangle scenario, where the sources vertices are omitted for readability. a) the original scenario, b) the 6-ring contains the inflation of Figure 3b as a subgraph, c) the 6-ring with subgraphs highlighted, in black a subgraph compatible with the original scenario, d) the 9-ring with a highlighted subgraph matching a subgraph of the 6-ring but not of the original scenario, e) a sketch of the 12-ring.

- *Parties receive a complete set of sources:*

$$(\mathcal{S}_i, \mathcal{O}_j) \in \mathcal{E} \Rightarrow \forall l, \exists k, (\mathcal{S}_i^{(k)}, \mathcal{O}_j^{(l)}) \in \mathcal{E}', \quad (25)$$

Additionally, if the inflation is *nonsignaling*, we impose the additional rule:

- *No duplication of sources:*

$$\{(\mathcal{S}_i^{(k)}, \mathcal{O}_j^{(l)}), (\mathcal{S}_i^{(k)}, \mathcal{O}_j^{(l')})\} \subset \mathcal{E}' \Rightarrow l = l'. \quad (26)$$

Such inflations are referred to as non-fanout [15]. In the triangle scenario, all the inflations have the shape of a ring, as outlined in Figure 4. The complete family of nonsignaling constraints is thus a sequence of rings containing $3n$ observers for $n = 2, 3, \dots$. The same reasoning applies to the square scenario, where the complete family of nonsignaling constraints is expressed by a sequence of rings of length $4n$ for $n = 2, 3, \dots$.

3.3 AI-expressible subsets

We consider subsets $\mathcal{K}' \subseteq \mathcal{I}'$ of observers in an inflation \mathcal{S}' . When $\mathcal{K}' = \{\mathcal{O}_j^{(l)}\}$ is a singleton, the

marginal probability distribution of the inflation scenario matches the marginal probability distribution \vec{P} of the original scenario:

$$\vec{P}_{\mathcal{O}_j^{(\ell)}}^{\text{inflation}} = \vec{P}_{\mathcal{O}_j}, \quad (27)$$

This works as well when $\mathcal{K}' = \{\mathcal{O}_j^{(\ell)}, \mathcal{O}_{j'}^{(\ell')}\}$ and one of the following holds true.

- There are sources connected to both $\mathcal{O}_j^{(\ell)}$ and $\mathcal{O}_{j'}^{(\ell')}$, but $j \neq j'$. We consider the subgraph of \mathbb{S}' after removal of the observers in $\mathcal{J}' \setminus \mathcal{K}'$ and of orphan sources (sources not connected to any observer). This subgraph matches the subgraph of the original scenario \mathbb{S} after removal of the observers in $\mathcal{J} \setminus \{\mathcal{O}_j, \mathcal{O}_{j'}\}$ and orphan sources. Thus

$$\vec{P}_{\mathcal{O}_j^{(\ell)} \mathcal{O}_{j'}^{(\ell')}}^{\text{inflation}}(xy) = \vec{P}_{\mathcal{O}_j \mathcal{O}_{j'}}(xy), \quad (28)$$

where x, y are enumerated over the possible outcomes. This corresponds to the cut inflation in Figure 3b, where $\vec{P}_{\mathcal{A}^{(1)} \mathcal{B}^{(1)}}(ab) = \vec{P}_{\mathcal{A} \mathcal{B}}(ab)$.

- There is no source \mathcal{S}_i^k connected to both $\mathcal{O}_j^{(\ell)}$ and $\mathcal{O}_{j'}^{(\ell')}$. Then

$$\begin{aligned} \vec{P}_{\mathcal{O}_j^{(\ell)} \mathcal{O}_{j'}^{(\ell')}}^{\text{inflation}}(xy) &= \vec{P}_{\mathcal{O}_j^{(\ell)}}^{\text{inflation}}(x) \vec{P}_{\mathcal{O}_{j'}^{(\ell')}}^{\text{inflation}}(y) \\ &= \vec{P}_{\mathcal{O}_j}(x) \vec{P}_{\mathcal{O}_{j'}}(y), \end{aligned} \quad (29)$$

again over all possible x, y . This corresponds to Figure 3c where $\vec{P}_{\mathcal{A}^{(1)} \mathcal{C}^{(1)}}(ac) = \vec{P}_{\mathcal{A}}(a) \vec{P}_{\mathcal{C}}(c)$

Such sets \mathcal{K}' are called *ai-expressible*, following [15]. The definition generalizes to any cardinality of \mathcal{K}' .

Definition 16. *Given an inflation \mathbb{S}' of a scenario \mathbb{S} , a subset $\mathcal{K}' \subseteq \mathcal{J}'$ of the observers is AI-expressible when the following holds: after removing the observers in $\mathcal{J}' \setminus \mathcal{K}'$ and orphan sources, the connected components of the resulting graph each match a subgraph of \mathbb{S} .*

For an AI-expressible set \mathcal{K}' , we $\mathcal{K}' = \mathcal{H}'_1 \cup \mathcal{H}'_2 \cup \dots \cup \mathcal{H}'_{|\mathcal{K}'|}$ as a disjoint union of observers for each of its connected components. For each \mathcal{H}'_h , we write \mathcal{H}_h the corresponding observers in the original scenario, after dropping the copy index. Then we identify:

$$\begin{aligned} P_{\mathcal{K}'}(\mathbf{k}) &= P_{\mathcal{H}'_1 \dots \mathcal{H}'_{|\mathcal{K}'|}}(\mathbf{h}_1 \dots \mathbf{h}_{|\mathcal{K}'|}) \\ &= P_{\mathcal{H}'_1}(\mathbf{h}_1) \dots P_{\mathcal{H}'_{|\mathcal{K}'|}}(\mathbf{h}_{|\mathcal{K}'|}) \\ &= P_{\mathcal{H}_1}(\mathbf{h}_1) \dots P_{\mathcal{H}_{|\mathcal{K}'|}}(\mathbf{h}_{|\mathcal{K}'|}), \end{aligned} \quad (30)$$

and remark that the r.h.s. of (30) is a member of the monomials \mathbf{M} according to Definition 13.

3.4 Algorithms to compute with nonsignaling constraints

We do not know of a technique that can test if a particular \vec{P}_{ABC} is nonsignaling or signaling-enabling.

There is a relaxation that uses linear programming (LP), described in [15]. It is a relaxation because we need to impose a cutoff on the complexity of the inflation (in the triangle, that would be the ring length); also because some nonlinear independence conditions cannot be expressed using LP. Given a distribution \vec{P}_{ABC} and a cutoff on the complexity of the inflation, we can get two results: the distribution is incompatible with this limited set of nonsignaling constraints, or the result is inconclusive.

Algorithm 1. *From [15]. Decide on an inflation of the original scenario. Identify maximal AI-expressible sets of observers. Write all constraints between marginals of $\vec{P}_{\text{inflation}}$ and the explicit values of the corresponding monomials in \mathbf{M} in the form of (30). When the linear program is infeasible, we can extract a polynomial inequality $I \in \mathbb{R}\mathbf{M}$ in the form (18) that certifies that $\vec{P}_{\text{test}} \notin \mathcal{N}$, along with a decomposition that allows the verification of the certificate without solving the linear program again.*

This relaxation quickly becomes expensive as the complexity of the inflation grows. However, if we study patterns instead of probability distributions, the problem simplifies. Indeed, the semiring $(\mathbb{P}, +, \cdot)$ is isomorphic to the Boolean algebra $(\{0, 1\}, \vee, \wedge)$: the resulting Boolean satisfiability problem can be solved efficiently using SAT solvers.

Algorithm 2. *Similar as Algorithm 1, but the equality constraints are written between marginals of $\vec{P}_{\text{inflation}} \in \mathbb{P}^{N'}$ and $\vec{P}_{\text{test}} \in \mathbb{P}^N$. It is also possible to incorporate independence conditions of the form $P_{\mathcal{A}^{(1)} \mathcal{C}^{(1)}}(a_1 c_1) = P_{\mathcal{A}^{(1)}}(a_1) P_{\mathcal{C}^{(1)}}(c_1)$. The resulting problem is solved by a SAT solver. Some SAT solvers support the extraction of a proof or infeasibility certificate; but this is an active domain of research [31].*

However, there is a simpler algorithm if we restrict ourselves to equality constraints where the right-hand side is deduced directly from the pattern under test.

Algorithm 3. *There is an algorithm that solves a relaxation of the $\vec{P}_{\text{test}} \in \mathcal{N}$ decision problem in $\mathcal{O}(m \cdot N')$ time and $\mathcal{O}(N')$ space, if m is the number of equality constraints and N' the number of elements in $\vec{P}_{\text{inflation}} \in \mathbb{P}^{N'}$.*

The general principle is to identify all coefficients $= \circlearrowleft$ in $\vec{P}_{\text{inflation}}$ using (8), then look for a contradiction using a constraint $= \checkmark$ using (9).

We discuss Algorithm 3 using the example of Section 3.1, where $\vec{P}_{\text{inflation}} = \vec{P}_{\mathcal{A}^{(1)} \mathcal{B}^{(1)} \mathcal{C}^{(1)}}$ and $\vec{P}_{\text{test}} =$

$(\checkmark, \circlearrowleft, \circlearrowleft, \circlearrowleft, \circlearrowleft, \circlearrowleft, \circlearrowleft, \checkmark)^\top$. We sort constraints according to the right-hand side:

$$\begin{aligned} P_{A^{(1)}B^{(1)}}(00) &= P_{A^{(1)}B^{(1)}}(11) = \checkmark \\ P_{B^{(1)}C^{(1)}}(00) &= P_{B^{(1)}C^{(1)}}(11) = \checkmark \\ P_{A^{(1)}C^{(1)}}(00) &= P_{A^{(1)}C^{(1)}}(01) = \checkmark \\ P_{A^{(1)}C^{(1)}}(10) &= P_{A^{(1)}C^{(1)}}(11) = \checkmark \end{aligned} \quad (31)$$

and

$$\begin{aligned} P_{A^{(1)}B^{(1)}}(01) &= P_{A^{(1)}B^{(1)}}(10) = \circlearrowleft \\ P_{B^{(1)}C^{(1)}}(01) &= P_{B^{(1)}C^{(1)}}(10) = \circlearrowleft. \end{aligned} \quad (32)$$

Let the hypothesis set $\mathbb{H} = \{\circlearrowleft, ?\}$ where \circlearrowleft means the same as in \mathbb{P} and $?$ is a placeholder for either \circlearrowleft or \checkmark . We initialize the hypothesis vector $\vec{H}_{\text{inflation}} \in \mathbb{H}^N$ as $\vec{H}_{\text{inflation}} := (?, \dots, ?)^\top$. Then, for each constraint with a right-hand side $= \circlearrowleft$, we identify the elements of $\vec{H}_{\text{inflation}}$ that correspond to the sum making up to the left-hand side. As $x + y + \dots = \circlearrowleft$ implies $x = y = \dots = \circlearrowleft$, we set all these elements to \circlearrowleft .

For example, $P_{A^{(1)}B^{(1)}}(01) = \circlearrowleft$ implies that $H_{\text{inflation}}(010) = H_{\text{inflation}}(011) = \circlearrowleft$. After running through all the constraints in (32), we get

$$\vec{H}_{\text{inflation}} = (?, \circlearrowleft, \circlearrowleft, \circlearrowleft, \circlearrowleft, \circlearrowleft, \circlearrowleft, ?)^\top. \quad (33)$$

Then, we scan the constraints with right-hand side $= \checkmark$. For each constraint, we identify the elements of $\vec{H}_{\text{inflation}}$ that correspond to the sum making up the left-hand side. If all these elements $= \circlearrowleft$, we get the contradiction we are looking for. For example

$$\begin{aligned} P_{A^{(1)}C^{(1)}}(01) &= P_{A^{(1)}B^{(1)}C^{(1)}}(001) + \\ &\quad + P_{A^{(1)}B^{(1)}C^{(1)}}(011) = \checkmark \end{aligned} \quad (34)$$

whereas

$$H_{A^{(1)}B^{(1)}C^{(1)}}(001) = H_{A^{(1)}B^{(1)}C^{(1)}}(011) = \circlearrowleft. \quad (35)$$

3.5 Possibilistic certificates

Such contradictions give rise to a special type of certificate.

Definition 17. A possibilistic certificate is written:

$$T \Rightarrow E_1 \vee E_2 \vee \dots \vee E_m \quad (36)$$

where each of T, E_1, \dots, E_m correspond to a valuation of the inflation scenario (see Definition 12) whose set of observers is AI-expressible. The valuation T is the antecedent and the valuations $\{E_i\}$ are the consequents. The statement means that if T happens, then at least one of the $\{E_i\}$ must happen.

We now describe how to extract a certificate from such a contradiction.

Algorithm 4. When Algorithm 3 succeeds, we can extract a polynomial inequality that can discriminate probability distributions that are close to the one of the pattern, but do not necessarily match a realization of the pattern.

We describe the algorithm below. From a possibilistic certificate (18), we deduce, using the union bound:

$$\begin{aligned} P(T) &\leq P(E_1 \vee \dots \vee E_m) \\ &\leq P(E_1) + \dots + P(E_m), \end{aligned} \quad (37)$$

thus, trivially, $P(T) \leq P(E_1) + \dots + P(E_m)$ at the pattern level. As the antecedent and consequents are AI-expressible, they all correspond to elements of \mathcal{M} that can be computed from the probability distribution of the original scenario.

As an example, we write the following certificate for the cut inflation of the triangle scenario: its validity is proven later.

$$\underbrace{(a^{(1)} = 0, c^{(1)} = 1)}_T \Rightarrow \underbrace{(a^{(1)} = 0, b^{(1)} = 1)}_{E_1} \vee \underbrace{(b^{(1)} = 0, c^{(1)} = 1)}_{E_2}. \quad (38)$$

We get:

$$P_{A^{(1)}C^{(1)}}(01) \leq P_{A^{(1)}B^{(1)}}(01) + P_{B^{(1)}C^{(1)}}(01). \quad (39)$$

Relating the inflation distribution with the original distribution, we have:

$$P_A(0)P_C(1) \leq P_{AB}(01) + P_{BC}(01), \quad (40)$$

$$P_A(0)P_C(1) \leq P_{AB}(01) + P_{BC}(01), \quad (41)$$

which is violated by GHZ-like distributions (22) both at the probability and possibilistic level.

How do we find such sets? One way is to post-process the result of the algorithm presented in Section 3.4.

Every valuation corresponds to a subset of indices in $\vec{P}_{\text{inflation}}$; we write the corresponding sets T, E_1, \dots, E_M ; when $T \subseteq E_1 \cup \dots \cup E_M$ the validity of the certificate easily follows. As a result of the algorithm, we saw that the constraint $P_{A^{(1)}C^{(1)}}(01) = \checkmark$ leads to a contradiction; this constraint provides the antecedent $T = \{001, 011\}$.

Where does this contradiction actually comes from? We present in Table 2 the indices in T and those of all the constraints that set elements to \circlearrowleft . Here, we naturally take $E_1 = \{010, 011\}$, $E_2 = \{001, 101\}$.

To strengthen the resulting inequality, we want to minimize the number of sets E_1, \dots, E_M that cover T ; this corresponds to the well known set cover problem [32].

a	b	c	$P_{A^{(1)}C^{(1)}}(01) = \checkmark$	$P_{A^{(1)}B^{(1)}}(01) = \emptyset$	$P_{A^{(1)}B^{(1)}}(10) = \emptyset$	$P_{B^{(1)}C^{(1)}}(01) = \emptyset$	$P_{B^{(1)}C^{(1)}}(10) = \emptyset$
0	0	0					
0	0	1	T			\emptyset	
0	1	0		\emptyset			\emptyset
0	1	1	T	\emptyset			
1	0	0			\emptyset		
1	0	1			\emptyset	\emptyset	
1	1	0					\emptyset
1	1	1					

Table 2: Investigation of a contradiction arising from the possibilistic algorithm of Section 3.4.

4 Local correlations

We now turn our attention to local correlations, which are obtained when the sources are modeled by local hidden variables. Each source \mathcal{S}_i is associated with a random variable $s_i \in \Omega_i$. Without loss of generality [33], we assume the sample space Ω_i to be finite, so that s_i has probability distribution $P_{s_i}(s_i)$.

In turn, we describe each observer using a probability distribution $P_{\mathcal{O}_j|s_{i_1,1} \dots s_{i_j,n_j}}(o_j|s_{i_1,1} \dots s_{i_j,n_j})$ where $i \in \{i_{j,1}, \dots, i_{j,n_j}\}$ if and only if $(\mathcal{S}_i, \mathcal{O}_j) \in \mathcal{E}$.

The resulting correlations are:

$$P(o_1 \dots o_{|\mathcal{J}|}) = \sum_{s_1, \dots, s_{|\mathcal{I}|}} P_{s_1}(s_1) \dots P_{s_{|\mathcal{I}|}}(s_{|\mathcal{I}|}) \cdot \prod_j P_{\mathcal{O}_j|s_{i_1,1} \dots s_{i_j,n_j}}(o_j|s_{i_1,1} \dots s_{i_j,n_j}). \quad (42)$$

Without loss of generality, we can assume $P_{s_i}(s_i) > 0$ for all i and s_i ; otherwise we can simply reduce the cardinality of the corresponding sources by removing the values that never happen.

Algorithm 5. As explicited in [33], the decision problem $\vec{P}_{\text{test}} \in \mathcal{L}$ reduces to a polynomial feasibility problem.

Consider the triangle scenario. If α, β, γ are classical random variables taken from the distributions $P_\alpha(\alpha)$, $P_\beta(\beta)$, $P_\gamma(\gamma)$, processed by the nodes A,B,C according to the probability distributions $P_A(a|\beta\gamma)$, $P_B(b|\gamma\alpha)$, $P_C(c|\alpha\beta)$, then the observed outcomes are

$$P(abc) = \sum_{\alpha\beta\gamma} P_\alpha(\alpha)P_\beta(\beta)P_\gamma(\gamma) \cdot P_A(a|\beta\gamma)P_B(b|\gamma\alpha)P_C(c|\alpha\beta). \quad (43)$$

We can always assume that α, β, γ are taken from finite sets, with $|\Omega_\alpha|, |\Omega_\beta|, |\Omega_\gamma| \leq 6$, according to [33]. The decision problem $\vec{P} \in \mathcal{L}$ reduces to a feasibility problem including $3 \cdot 5$ degrees of freedom for the distribution of the classical random variables, and $3 \cdot 36$ degrees of freedom for the nodes processing distributions P_A, P_B, P_C . Such nonconvex and highly nonlinear feasibility problems are usually difficult to handle on their own.

However, looking for a model at the level of patterns is easier.

Algorithm 6. To find whether a pattern \vec{P}_{test} has a model, we collapse the model elements to possibilistic distributions. We apply the morphism φ of Section 2.1 to (42) and get:

$$\begin{aligned} & P(o_1 \dots o_{|\mathcal{J}|}) \\ &= \sum_{s_1, \dots, s_{|\mathcal{I}|}} P_{s_1}(s_1) \dots P_{s_{|\mathcal{I}|}}(s_{|\mathcal{I}|}) \cdot \\ & \quad \cdot \prod_j P_{\mathcal{O}_j|s_{i_1,1} \dots s_{i_j,n_j}}(o_j|s_{i_1,1} \dots s_{i_j,n_j}) \\ &= \sum_{\mathbf{s}} \prod_j P_{\mathcal{O}_j|s_{i_1,1} \dots s_{i_j,n_j}}(o_j|s_{i_1,1} \dots s_{i_j,n_j}). \quad (44) \end{aligned}$$

This feasibility problem can be solved using a SAT solver.

In the triangle scenario, those are $P_\alpha, P_\beta, P_\gamma, P_A, P_B, P_C$. Without loss of generality, we have $P_\alpha(\alpha) = P_\beta(\beta) = P_\gamma(\gamma) = \checkmark$, and such the distribution of the sources can be omitted from the model. The equation (43) reduces to:

$$P(abc) = \sum_{\alpha\beta\gamma} P_A(a|\beta\gamma)P_B(b|\gamma\alpha)P_C(c|\alpha\beta) \quad (45)$$

We mentioned the inflation technique in the context of the characterization of the nonsignaling set \mathcal{N} , where a complete set of constraints is obtained by applying rules (24) (26). Now, keeping (24), (25) but no longer requiring (26), we use the fact that classical information can be copied. As with Algorithm 1, the resulting feasibility problem is a linear program. However, there is a systematic way of constructing a complete hierarchy of such relaxations.

Algorithm 7. A complete hierarchy of relaxations for the decision problem $\vec{P} \in \mathcal{L}$ is obtained by constructing the following sequence of inflations [34]. For a given n , we include n copies of each source, and add as many copies of observers as possible saturating conditions (24) and (25); this is known as the web inflation.

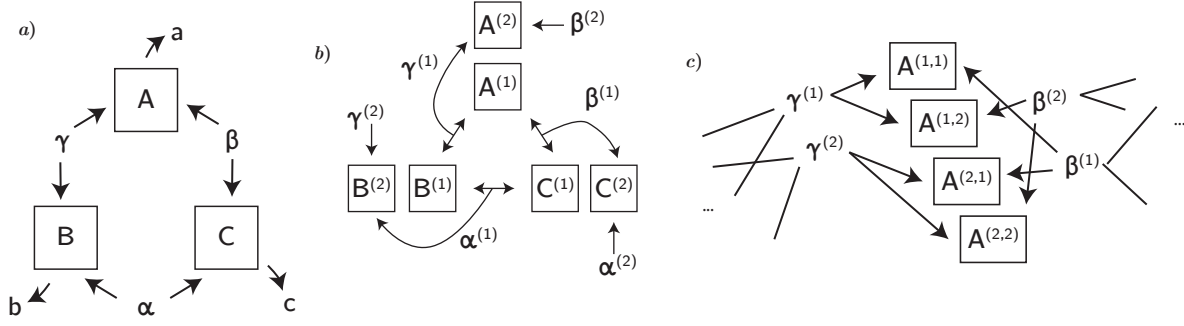


Figure 5: In a), the triangle scenario composed of three devices (A, B, C) and three sources (α, β, γ). In b), the spiral inflation already mentioned in [15]. In c), part of the web inflation for $n = 2$ copies of the sources, where copies of A are indexed according to the source copy index.

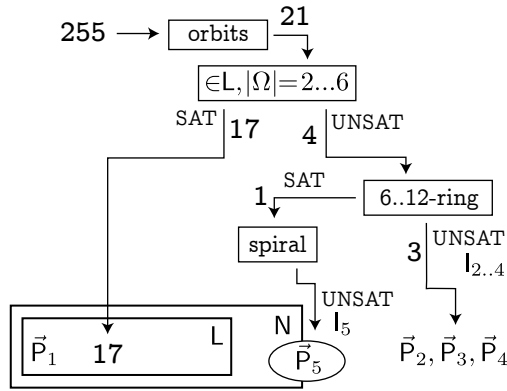


Figure 6: Classification of the patterns/orbits in the triangle scenario. For details, see main text.

In Figure 5, we display different inflations for the triangle scenario. As before, a variant of Algorithm 7 applies to patterns.

Algorithm 8. *The inflation technique applies for patterns as well, using either a SAT solver as in Algorithm 2 or filling a bit vector as in Algorithm 3.*

There is an additional and often faster algorithm to decide whether a pattern is local or not.

Algorithm 9. *The possible worlds technique introduced by Fraser in [26] considers the combinatorics of assigning definite valuations to hidden variables, and solves the local set decision problem.*

5 Triangle scenario: results

We come back to the triangle scenario of Section 2.3. After reduction under symmetry and normalization, we test all 21 orbits. Our classification is summarized in Figure 6.

5.1 Patterns in L

We apply Algorithm 6 with cardinality 6, which provides a local model if such a model exists [33]. We find that 17 out of 21 orbits have a local model. We repeat Algorithm 6 with cardinality 2. Interestingly the results are the same: thus there is no pattern in L that requires a source alphabet of cardinality more than 2, which is the minimum (cardinality 1 corresponds to a source being omitted). Representatives of those 17 orbits are given in Appendix A. These include $P_{\checkmark} = [000] + [001] + [010] + [011] + [100] + [101] + [110] + [111]$ (in all scenarios, the all- \checkmark pattern is always local!), the deterministic pattern $P_{[111]} = [111]$, and the pattern

$$P_1 = [000] + [001] + [010] + [100]. \quad (46)$$

The four patterns not in L are:

$$\begin{aligned} P_2 &= [011] + [100], \\ P_3 &= [011] + [100] + [111], \\ P_4 &= [011] + [100] + [110] + [111], \\ P_5 &= [001] + [010] + [100], \end{aligned} \quad (47)$$

noting that P_2 is in the orbit $(\vec{P}^{\text{GHZ}})^G$, cf. (23). The pattern P_5 corresponds to the pattern of a W -type distribution.

5.2 Patterns not in N

Using Algorithm 3 and the 6-ring inflation, we found that P_2, P_3 and P_4 are signaling enabling. We then increased the relaxation degree to the 9-ring and 12-ring, and do not find that P_5 is signaling enabling. Is it surprising? We note that $3n$ -ring inflations only match subgraphs that contain one or two observers nodes: $P_A, P_B, P_C, P_{AB}, P_{AC}, P_{BC}$. On those marginals, P_5 is indistinguishable from P_1 , and $P_1 \in N$ follows from $P_1 \in L$.

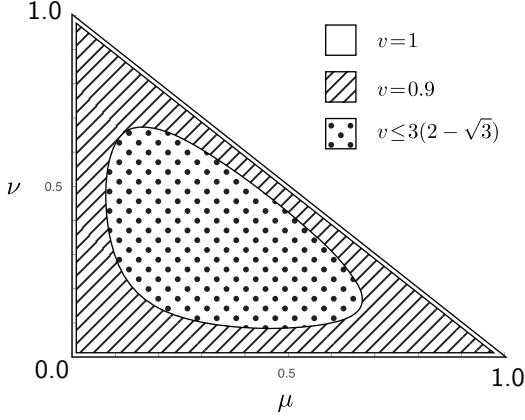


Figure 7: For $v = 1$, it seems that only a thin region around the triangle is feasible for the 6-ring inflation. As the visibility v decreases, this region grows: for $v = 9$, it contains the border and the dashed region. When $v \leq 3(2 - \sqrt{3}) \cong 0.804$, the whole triangle satisfies the 6-ring inflation.

5.3 Polynomial inequalities from possibilistic results

Using Algorithm 4 and the 6-ring inflation, we found the following polynomial inequalities, which are respectively violated by P_2 , P_3 and P_4 .

$$I_2 = P_{AC}(11)P_A(0) + P_{BC}(10)P_B(0) - P_{AB}(01)P_{AB}(10) \geq 0, \quad (48)$$

$$I_3 = P_{AC}(00)P_{AC}(11) + P_{BC}(01)P_B(1) + P_{BC}(10)P_{BC}(00) - P_{AB}(01)P_{AB}(10) \geq 0, \quad (49)$$

$$I_4 = P_{AC}(00)P_A(1) + P_{BC}(01)P_B(1) - P_{AB}(01)P_{AB}(10) \geq 0. \quad (50)$$

The pattern P_5 is detected by the spiral inflation of Figure 5c, and Algorithm 4 gives the inequality:

$$I_5 = P_{ABC}(000) + P_{AB}(11)P_C(1) + P_{AC}(11)P_B(1) + P_{BC}(11)P_A(1) - P_A(1)P_B(1)P_C(1) \geq 0. \quad (51)$$

However, that certifies that $P_5 \notin \mathcal{L}$, the status of this orbit regarding the nonsignaling set is unclear.

5.4 The case of the W -type distribution

We then test whether *realizations* $\vec{P}_5^{(a,b)}$ of the pattern P_5 are in \mathcal{N} , using Algorithm 1:

$$\vec{P}_5^{(\mu,\nu)} = \mu[001] + \nu[010] + (1 - \mu - \nu)[100], \quad (52)$$

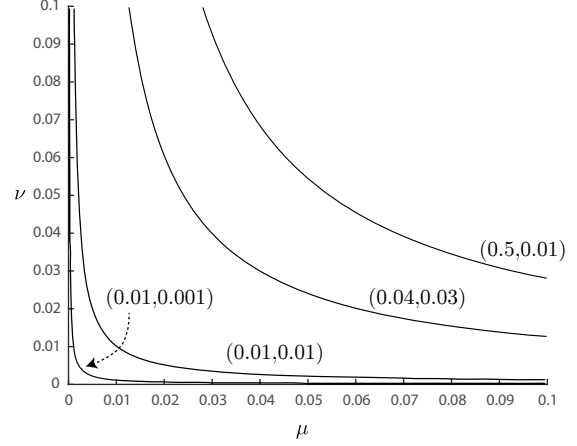


Figure 8: Certificates found by solving the 6-ring inflation LP for $P_5^{(\mu_0, \nu_0)}$ according to four pairs (μ_0, ν_0) , shown along the certificates.

where $0 < \mu, \nu, (1 - \mu - \nu) < 1$, possibly including noise with visibility v :

$$P_5^{(\mu, \nu, v)}(abc) = vP_5^{(\mu, \nu)}(abc) + (1 - v)/8. \quad (53)$$

In Figure 7, for $v = 1$, it seems at first sight that most of the considered area is not in \mathcal{N} ; at $v \leq 3(2 - \sqrt{3})$, all of it is feasible. By solving the linear program of Algorithm 1 closer and closer to the border, it becomes clear that the feasible region has a certain thickness in the neighborhood of the border. While the linear program becomes more and more numerically unstable, we can use exact arithmetic and extract infeasibility certificates. We plot the results in Figure 8.

While we could not rule out the pattern P_5 using the possibilistic semiring, it may well be that all its realizations are ruled out by using Algorithm 1 on a suitable $3n$ -ring inflation. We leave that question as an open problem.

6 Square scenario: results

We address the square scenario with binary outcomes, as shown in Figure 1 and in Figure 10a. Our classification process is summarized in Figure 9. First, the patterns group into 804 orbits under symmetry. We then verify if the pattern obeys the factorization condition:

$$P_{AC}(ac) = P_A(a)P_C(c), P_{BD}(bd) = P_B(b)P_D(d), \quad (54)$$

which should always be satisfied: 285 orbits fail this test and can be pruned. There remains 519 interesting patterns to classify.

6.1 Patterns in \mathcal{L}

Applying the results of [33], all local models use classical random variables with an alphabet size of at most

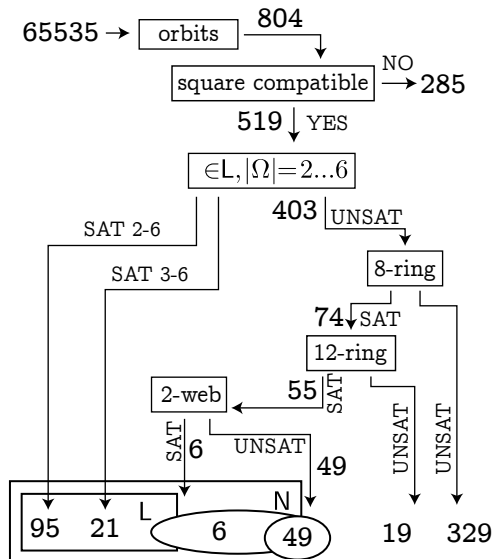


Figure 9: Classification of patterns/orbits in the square scenario, see main text for the process.

12. Due to computational constraints, we could only run Algorithm 6 with alphabet size up to 6. For 95 orbits, we found a model using alphabet size 2. For 21 additional orbits, we found a model using alphabet size 3. Increasing the alphabet size from 3 to 6 did not help further.

For the remaining 403 orbits, we cannot rule out the possibility of a model for an alphabet size from 7 to 12. We turn to the possibilistic inflation technique.

6.2 Patterns not in N

We applied Algorithm 2 on those 403 orbits using two different nonsignaling inflations: the 8-ring and the 12-ring, corresponding to the inflations in Figure 10b and Figure 10c respectively. The 8-ring finds 329 orbits to be signaling-enabling, while the 12-ring finds 19 additional orbits that are also signaling-enabling. We are left with 55 orbits whose status is yet unknown. We then apply the local 2-web inflation, as described in Figure 5c and Figure 10d, with two copies of each source. We have 49 patterns that failed to satisfy the 2-web inflation: for sure, those patterns are $\notin L$, but their membership status regarding N is unknown. Remains 6 patterns that satisfy the 2-web inflation. At that point, we turn to the possible worlds technique (Algorithm 9) and find that those 6 patterns are $\notin L$. In particular, this means that all the patterns in L can be realized with models of LHV cardinality 3.

6.3 Quantum nonlocality in the square network

Interestingly, the characterisation of patterns that are nonlocal, i.e. not in L, allows us to provide a simple example of a quantum nonlocal distribution in the

square network. Of particular interest is the fact the low cardinality of the outcomes, which are all binary (while there are no inputs). Note that it is still an open question whether nonlocality is possible in the triangle network with binary outputs and no inputs, see e.g. [10].

The construction is based on the well-known Hardy paradox [23], a demonstration of standard quantum Bell nonlocality based on a possibilistic argument. We start with a standard bipartite Bell test. The first party (Alice) receives a binary input x (from another party called Dave) and provides a binary output a . Similarly, the second party (Bob) receives a binary input y (from Charlie) and outputs a bit b . One usually considers the conditional joint probability $P(ab|xy)$. In Hardy's construction, Alice and Bob perform well-chosen local Pauli measurements on a non-maximally entangled state of two-qubits, see [23] for details. The key point is that the resulting probability distribution has the following feature:

$$P(10|10) = P(01|01) = P(00|11) = 0 \quad (55)$$

while all other probabilities are strictly positive, including $P(00|00)$, which leads to a logical contradiction for any local model.

Now we embed this bipartite Bell test in the square network, adapting the idea of Fritz [3]. We place Alice, Bob, Charlie and Dave in a square network. The source connecting Alice and Bob distributes the required two-qubit entangled state. The source between Alice and Dave distributes the inputs x , while the source between Bob and Charlie distributes the input y . Note that the source between Charlie and Dave is here useless. Alice and Bob output a and b , respectively. Charlie and Dave output y and x , respectively. We obtain a quantum distribution on the square with binary outputs. Using the SAT algorithm, it can be checked that the pattern of this quantum distribution is not in L.

This shows that the square network with binary outputs allows for quantum nonlocality. We note that a similar construction shows that when Alice and Bob share a Popescu-Rohrlich nonlocal box [35], the resulting pattern is not in L. This suggests that the square network with binary output could also feature stronger than quantum nonlocality.

7 Relaxation of the independence assumption

The study of nonlocality in networks assumes that sources are perfectly independent

$$\begin{aligned} P_{\mathbf{s}}(\mathbf{s}) &= P_{s_1 \dots s_{|\mathcal{I}|}}(s_1 \dots s_{|\mathcal{I}|}) \\ &= P_{s_1}(s_1) \dots P_{s_{|\mathcal{I}|}}(s_{|\mathcal{I}|}) = \prod_{i \in \mathcal{I}} P_{s_i}(s_i) \end{aligned} \quad (56)$$

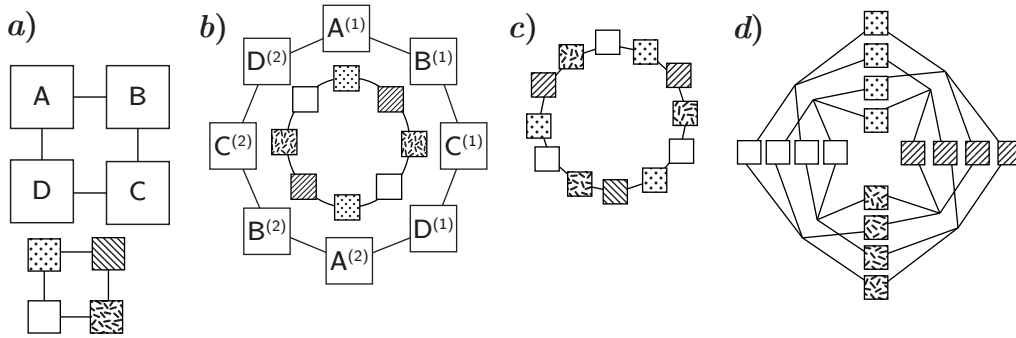


Figure 10: a) Square scenario, including simplified drawing. b) 8-ring inflation, including simplified drawing. c) Simplified drawing of the 12-ring inflation. d) Simplified drawing of the 2-web inflation.

whereas recent works have challenged this assumption by considering that the sources in the network could be classically correlated [36] (see also [37]). In this section, we extend inequalities obtained through Algorithm 4 to be still valid when the independence assumption is relaxed. We model the correlations among the $\{s_i\}$ by introducing another random variable $\lambda = 1, \dots, \Lambda$ distributed according to $P(\lambda)$, as in Figure 11. Since the original sources in the network may be affected by the latter, we need to bound its causal influence to avoid that any distribution $P_{\mathcal{O}|\mathbf{s}}$ can be reproduced via a local model by setting ($s_1 = \dots = s_{|\mathcal{I}|} = \lambda$) with λ sampled from $P_{\mathcal{O}|\mathbf{s}}$. We therefore impose the condition

$$\epsilon_1 \prod_{i \in \mathcal{I}} P_{s_i}(s_i) \leq P_{\mathbf{s}|\lambda}(\mathbf{s}|\lambda) \quad (57)$$

for some $\epsilon_1 \in (0, 1]$. Without loss of generality, we require $P(\lambda) > 0$. We write \mathcal{L}_{ϵ_1} the set of probability distributions satisfying a relaxed condition similar to (42):

$$P(o_1 \dots o_{|\mathcal{J}|}) = \sum_{\lambda} P(\lambda) \sum_{\mathbf{s}} P_{\mathbf{s}|\lambda}(\mathbf{s}|\lambda) \cdot \prod_j P_{\mathcal{O}_j|s_{i_{j,1}} \dots s_{i_{j,n_j}}}(o_j | s_{i_{j,1}} \dots s_{i_{j,n_j}}). \quad (58)$$

Similarly, we write \mathcal{L}_{ϵ_1} the set of patterns achievable with a given ϵ_1 . For $\epsilon_1 = 1$, we get back $\mathcal{L}_{\epsilon_1} = \mathcal{L}$, while for $\epsilon_1 = 0$, any normalized \vec{P} can be reached by embedding the desired outcomes in $\lambda = (o_1, \dots, o_{|\mathcal{I}|})$ and passing the relevant values through the sources.

We make an interesting observation in the intermediate regime.

Proposition 1. *For $0 < \epsilon_1 < 1$, we have $\mathcal{L}_{\epsilon_1} = \mathcal{L}$. Thus, if a pattern is not local, it is not local even in the presence in limited correlation between the sources.*

Proof. We apply the semiring morphism $\varphi : \mathbb{R}^{\geq 0} \rightarrow \mathbb{P}$

of Section 2.1 to Eq. (58) to obtain:

$$\begin{aligned} P(o_1 \dots o_{|\mathcal{J}|}) &= \sum_{\lambda} P(\lambda) \sum_{\mathbf{s}} P_{\mathbf{s}|\lambda}(\mathbf{s}|\lambda) \cdot \\ &\quad \cdot \prod_j P_{\mathcal{O}_j|s_{i_{j,1}} \dots s_{i_{j,n_j}}}(o_j | s_{i_{j,1}} \dots s_{i_{j,n_j}}) \\ &= \sum_{\lambda} \sum_{\mathbf{s}} \prod_j P_{\mathcal{O}_j|s_{i_{j,1}} \dots s_{i_{j,n_j}}}(o_j | s_{i_{j,1}} \dots s_{i_{j,n_j}}) \\ &= \sum_{\mathbf{s}} \prod_j P_{\mathcal{O}_j|s_{i_{j,1}} \dots s_{i_{j,n_j}}}(o_j | s_{i_{j,1}} \dots s_{i_{j,n_j}}) \quad (59) \end{aligned}$$

where we made use of $P_{\mathbf{s}}(\mathbf{s}) = \checkmark$ for all \mathbf{s} by assumption, and $\epsilon_1 \prod_{i \in \mathcal{I}} P_{s_i}(s_i) \leq P_{\mathbf{s}|\lambda}(\mathbf{s}|\lambda)$ implies $P_{\mathbf{s}|\lambda}(\mathbf{s}|\lambda) = \checkmark$ for all \mathbf{s}, λ . The final equation is identical to Eq. (44), and thus the feasible sets are the same. \square

In essence, the condition $\epsilon_1 > 0$ limits the strength of the “common cause” λ correlating the sources so that it cannot veto a particular possible value assignment.

7.1 Inequalities with relaxation of the independence condition

Due to the noise present in experimental observations, it is desirable to derive inequalities that can certify that $\vec{P} \notin \mathcal{L}$ when the observed \vec{P} is close but does not conform to a particular pattern, in the presence of some amount of correlation between sources.

As a consequence of (57) we derive the following upper bound on the correlations between the sources, preventing from deterministic assignments of the sources $\{s_i\}$,

$$P_{\mathbf{s}|\lambda}(\mathbf{s}|\lambda) \leq \epsilon_2 \prod_{i \in \mathcal{I}} P_{s_i}(s_i) \quad (60)$$

for some $\epsilon_2 > 1$, which can be deduced from the value of $\epsilon_1 > 0$. Note that $\epsilon_2 = 1$ would lead to $\mathcal{L}_{\epsilon_1, \epsilon_2} = \mathcal{L}$.

We consider probabilistic inequalities derived from possibilistic certificates of the form (36), obtained first

without relaxing the independence condition. They are written according to valuations of the inflation scenario:

$$\begin{aligned} P(T) &\leq P(E_1 \vee \dots \vee E_m) \\ &\leq P(E_1) + \dots + P(E_m). \end{aligned} \quad (61)$$

All of these valuations are AI-expressible, meaning that they correspond to monomials in \mathbf{M} , which we write $M_T, M_{E_1}, \dots, M_{E_m}$. We write the monomial value evaluated on a test distribution \vec{P} as $M_T(\vec{P})$, etc.

The original inequality assuming independence of sources is written:

$$M_T(\vec{P}) \leq M_{E_1}(\vec{P}) + \dots + M_{E_m}(\vec{P}). \quad (62)$$

Consider $P(V)$ where V is a valuation AI-expressible in the inflation scenario. It corresponds to a monomial $M_V \in \mathbf{M}$ that can be computed from the probability distribution of the original scenario. Abusing the notation, we write $\deg V = \deg M_V$ the number of connected components in the subgraph containing as observers only the one occurring in the valuation.

Now, sources in the inflation scenario can be correlated through λ , as shown in Figure 11.

Lemma 1. *Let V be a AI-expressible valuation. Then, there exists a n such that:*

$$\epsilon_1^n M_V(\vec{P}_{\text{original}}) \leq P(V) \leq \epsilon_2^n M_V(\vec{P}_{\text{original}}) \quad (63)$$

Proof. Let V_1, \dots, V_N be the valuations of the connected components in the inflation subgraph addressed by V , and $M_{V_1}, \dots, M_{V_N} \in \mathbf{M}$ the corresponding monomials in the coefficients of the original probability distribution. We have

$$\begin{aligned} P(V) &= \sum_{\lambda, \mathbf{s}} P(\lambda) P(\mathbf{s}^{(1)}|\lambda) \dots P(\mathbf{s}^{(M)}|\lambda) \cdot \\ &\quad P(V_1|\mathbf{s}_{V_1}) \dots P(V_N|\mathbf{s}_{V_N}), \end{aligned} \quad (64)$$

where $\mathbf{s}^{(1)}, \dots, \mathbf{s}^{(n)}$, for a given n , are the n copies of sources present in the inflation (without loss of generality, we allow source copies not connected to any observer), and \mathbf{s}_{V_ℓ} regroups the sources needed to compute the outcome values present in the valuation component V_ℓ .

The connected components V_1, \dots, V_N are connected to distinct sources, and contain at most one copy of each original source, as all the components are AI-expressible. Without modifying $P(V)$, we relabel sources so that \mathbf{s}_{V_1} contains only sources of the form $\mathcal{S}_i^{(1)}$, \mathbf{s}_{V_2} contains only sources of the form $\mathcal{S}_i^{(2)}$ and so on. We have:

$$\begin{aligned} P(V) &= \sum_{\lambda} P(\lambda) \left[\sum_{\mathbf{s}_{V_1}} P(\mathbf{s}_{V_1}|\lambda) P(V_1|\mathbf{s}_{V_1}) \right] \dots \\ &\quad \dots \left[\sum_{\mathbf{s}_{V_N}} P(\mathbf{s}_{V_N}|\lambda) P(V_N|\mathbf{s}_{V_N}) \right]. \end{aligned} \quad (65)$$

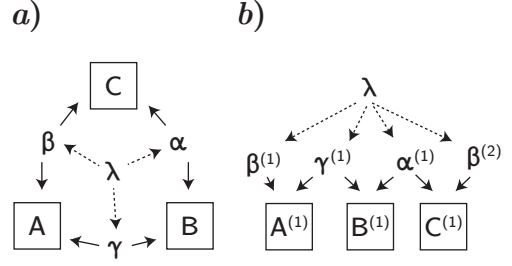


Figure 11: Relaxing the independence assumption in the triangle scenario

We now apply (57) and (60) to each term $\sum_{\mathbf{s}_{V_\ell}} P(\mathbf{s}_{V_\ell}|\lambda) P(V_\ell|\mathbf{s}_{V_\ell})$ and obtain:

$$\begin{aligned} \epsilon_1 M_\ell(\vec{P}_{\text{original}}) &\leq \sum_{\mathbf{s}_{V_\ell}} P(\mathbf{s}_{V_\ell}|\lambda) P(V_\ell|\mathbf{s}_{V_\ell}) \\ &\leq \epsilon_2 M_\ell(\vec{P}_{\text{original}}) \end{aligned} \quad (66)$$

and thus:

$$\epsilon_1^n M_V(\vec{P}_{\text{original}}) \leq P(V) \leq \epsilon_2^n M_V(\vec{P}_{\text{original}}). \quad (67)$$

□

Using this last lemma, we are ready to write an inequality valid in presence of correlations between sources:

$$\begin{aligned} \epsilon_1^n M_T(\vec{P}) &\leq P(T) \\ &\leq P(E_1) + \dots + P(E_m) \\ &\leq \epsilon_2^n [M_{E_1}(\vec{P}) + \dots + M_{E_m}(\vec{P})]. \end{aligned} \quad (68)$$

As an example, the inequality (40) comes from a certificate of the form (18) which is interpreted probabilistically as (39):

$$P_{A^{(1)}C^{(1)}}(01) \leq P_{A^{(1)}B^{(1)}}(01) + P_{B^{(1)}C^{(1)}}(01), \quad (69)$$

and translates to

$$(\epsilon_1)^2 P_A(0) P_C(1) \leq \epsilon_2 [P_{AB}(01) + P_{BC}(01)]. \quad (70)$$

8 Conclusion

We explored the possibilistic approach to network locality. We derived efficient algorithms to test whether a given possibilistic pattern is compatible with local (classical) or nonsignaling resources. We also considered the action of the symmetries of the scenario on those patterns to group them into orbits as to simplify the problem and hence reduce its computational costs.

In turn, we applied these methods to the triangle and square networks. In the case of the triangle network with binary outcomes, most of the orbits are

local, and we could find explicit local models using binary classical variables. We found that three orbits were signaling-enabling (hence incompatible with the triangle network), while the orbit corresponding to the so-called “W pattern” exhibits an interesting feature. It cannot be revealed as signaling-enabling, however, it seems that the vast majority of its realizations are indeed signaling-enabling at a low ring inflation level. This is our first open question: can any realization of the W pattern be detected (as signaling enabling) by a ring inflation?

In the case of the square network with binary outcomes, the majority of patterns is signaling enabling; some of the patterns do not even respect the independence relation between observers. We listed the 116 patterns that are compatible with a local model, and found that all of them can be reached with local variables of cardinality 3 at most. Additionally, there are 55 patterns which are provably nonlocal, yet we do not know if they are non-signaling. This ambiguity is a fundamental limit of the current algorithms: we can find whether $\vec{P} \notin \mathbf{N}$, but we do not have an algorithm to construct models of $\vec{P} \in \mathbf{N}$. This is our second open question.

As an application of our methods, we provided an example of quantum nonlocality in the square network with binary outcomes. This represents an instance of a quantum nonlocal distribution with low output cardinality. Are there nonlocal patterns in other orbits that have nevertheless a quantum realization?

Finally, we described how the inequalities recovered from possibilistic certificates are robust against correlations between the sources, relaxing the independence condition typically used in network locality. It would be interesting to see if this approach can be generalized to correlations between non-signaling sources.

As future avenues for research, there are natural scenarios to consider next under the possibilistic angle: other topologies, going beyond binary outcomes, adding inputs (different measurement settings) to the observers. However, even with the reduction coming from the grouping into orbits, the number of orbits will be pretty large. In the triangle scenario, the most interesting patterns, such as the W pattern, were also the patterns symmetrical under permutation of parties. Would it be then interesting in those scenarios to study a subset of orbits obeying a particular symmetry?

Acknowledgements.— We thank Elie Wolfe for bringing to our attention the possible worlds technique of Ref. [26] and sharing his code implementation, as well as for comments on a first version of this manuscript. We also thank Jean-Daniel Bancal, Marie Ioannou and Eloïc Vallée for discussions. We acknowledge financial support from the Swiss National Science Foundation (project 2000021_192244/1 and NCCR SwissMAP) and from

the European Union’s Horizon 2020 research and innovation program under the Marie Skłodowska-Curie grant agreement No 956071.

A Triangle patterns generation and classification

Source code available at <https://github.com/Possibilistic-network-nonlocality/main/tree/main/triangle%20scenario>

B Square patterns generation and classification

Source code available at <https://github.com/Possibilistic-network-nonlocality/main/tree/main/square%20scenario>

References

- [1] Armin Tavakoli, Alejandro Pozas-Kerstjens, Ming-Xing Luo, and Marc-Olivier Renou. “Bell nonlocality in networks”. *Reports on Progress in Physics* **85**, 056001 (2022).
- [2] C. Branciard, N. Gisin, and S. Pironio. “Characterizing the nonlocal correlations created via entanglement swapping”. *Phys. Rev. Lett.* **104**, 170401 (2010).
- [3] Tobias Fritz. “Beyond Bell’s theorem: correlation scenarios”. *New Journal of Physics* **14**, 103001 (2012).
- [4] Cyril Branciard, Denis Rosset, Nicolas Gisin, and Stefano Pironio. “Bilocal versus nonbilocal correlations in entanglement-swapping experiments”. *Physical Review A* **85** (2012).
- [5] Thomas C Fraser and Elie Wolfe. “Causal compatibility inequalities admitting quantum violations in the triangle structure”. *Physical Review A* **98**, 022113 (2018).
- [6] Marc-Olivier Renou, Elisa Bäumer, Sadra Boreiri, Nicolas Brunner, Nicolas Gisin, and Salman Beigi. “Genuine quantum nonlocality in the triangle network”. *Physical Review Letters* **123** (2019).
- [7] Marc-Olivier Renou and Salman Beigi. “Nonlocality for generic networks”. *Phys. Rev. Lett.* **128**, 060401 (2022).
- [8] Nicolas Gisin. “Entanglement 25 years after quantum teleportation: Testing joint measurements in quantum networks”. *Entropy* **21**, 325 (2019).
- [9] Paolo Abiuso, Tamás Kriváchy, Emanuel Cristian Boghiu, Marc-Olivier Renou, Alejandro Pozas-Kerstjens, and Antonio Acín. “Single-photon nonlocality in quantum networks”. *Phys. Rev. Research* **4**, L012041 (2022).

- [10] Sadra Boreiri, Antoine Girardin, Bora Ulu, Patryk Lypka-Bartosik, Nicolas Brunner, and Pavel Sekatski. “Towards a minimal example of quantum nonlocality without inputs” (2022).
- [11] Ivan Šupić, Jean-Daniel Bancal, Yu Cai, and Nicolas Brunner. “Genuine network quantum nonlocality and self-testing”. *Phys. Rev. A* **105**, 022206 (2022).
- [12] Ivan Supic and Nicolas Brunner. “Self-testing nonlocality without entanglement” (2022).
- [13] Rafael Chaves, Christian Majenz, and David Gross. “Information–theoretic implications of quantum causal structures”. *Nature Communications* **6** (2015).
- [14] Denis Rosset, Cyril Branciard, Tomer Jack Barnea, Gilles Pütz, Nicolas Brunner, and Nicolas Gisin. “Nonlinear bell inequalities tailored for quantum networks”. *Phys. Rev. Lett.* **116**, 010403 (2016).
- [15] Elie Wolfe, Robert W. Spekkens, and Tobias Fritz. “The Inflation Technique for Causal Inference with Latent Variables”. *Journal of Causal Inference* **7** (2019).
- [16] Miguel Navascués and Elie Wolfe. “The inflation technique completely solves the causal compatibility problem” (2017). [arXiv:1707.06476](https://arxiv.org/abs/1707.06476).
- [17] Mirjam Weilenmann and Roger Colbeck. “Non-shannon inequalities in the entropy vector approach to causal structures”. *Quantum* **2**, 57 (2018).
- [18] Johan Åberg, Ranieri Nery, Cristhiano Duarte, and Rafael Chaves. “Semidefinite tests for quantum network topologies”. *Phys. Rev. Lett.* **125**, 110505 (2020).
- [19] Elie Wolfe, Alejandro Pozas-Kerstjens, Matan Grinberg, Denis Rosset, Antonio Acín, and Miguel Navascués. “Quantum inflation: A general approach to quantum causal compatibility”. *Phys. Rev. X* **11**, 021043 (2021).
- [20] Tamás Kriváchy, Yu Cai, Daniel Cavalcanti, Arash Tavakoli, Nicolas Gisin, and Nicolas Brunner. “A neural network oracle for quantum nonlocality problems in networks”. *npj Quantum Information* **6**, 1–7 (2020).
- [21] Joe Henson, Raymond Lal, and Matthew F Pusey. “Theory-independent limits on correlations from generalized bayesian networks”. *New Journal of Physics* **16**, 113043 (2014).
- [22] Nicolas Gisin, Jean-Daniel Bancal, Yu Cai, Patrick Remy, Armin Tavakoli, Emmanuel Zambrini Cruzeiro, Sandu Popescu, and Nicolas Brunner. “Constraints on nonlocality in networks from no-signaling and independence”. *Nature Communications* **11**, 1–6 (2020).
- [23] Lucien Hardy. “Nonlocality for two particles without inequalities for almost all entangled states”. *Phys. Rev. Lett.* **71**, 1665–1668 (1993).
- [24] Daniel M. Greenberger, Michael A. Horne, Abner Shimony, and Anton Zeilinger. “Bell’s theorem without inequalities”. *American Journal of Physics* **58**, 1131–1143 (1990).
- [25] N. David Mermin. “Quantum mysteries revisited”. *American Journal of Physics* **58**, 731–734 (1990).
- [26] Thomas C. Fraser. “A combinatorial solution to causal compatibility”. *Journal of Causal Inference* **8**, 22–53 (2020).
- [27] Ivan Šupić, Jean-Daniel Bancal, and Nicolas Brunner. “Quantum nonlocality in networks can be demonstrated with an arbitrarily small level of independence between the sources”. *Phys. Rev. Lett.* **125**, 240403 (2020).
- [28] Yeong-Cherng Liang and Andrew C. Doherty. “Bounds on quantum correlations in Bell-inequality experiments”. *Physical Review A* **75**, 042103 (2007).
- [29] Elie Wolfe, Alejandro Pozas-Kerstjens, Matan Grinberg, Denis Rosset, Antonio Acín, and Miguel Navascués. “Quantum Inflation: A General Approach to Quantum Causal Compatibility”. *Physical Review X* **11**, 021043 (2021).
- [30] Laurens T. Ligthart, Mariami Gachechiladze, and David Gross. “A convergent inflation hierarchy for quantum causal structures” (2021). [arXiv:2110.14659](https://arxiv.org/abs/2110.14659).
- [31] Seulkee Baek, Mario Carneiro, and Marijn J. H. Heule. “A Flexible Proof Format for SAT Solver-Elaborator Communication”. In Jan Friso Groote and Kim Guldstrand Larsen, editors, *Tools and Algorithms for the Construction and Analysis of Systems*. Pages 59–75. *Lecture Notes in Computer Science* Cham (2021). Springer International Publishing.
- [32] Bernhard Korte. “Combinatorial optimization”. *Algorithms and combinatorics*. Springer. New York, NY (2012). 5 edition.
- [33] Denis Rosset, Nicolas Gisin, and Elie Wolfe. “Universal bound on the cardinality of local hidden variables in networks”. *Quantum Information & Computation* **18**, 910–926 (2018).
- [34] Miguel Navascués and Elie Wolfe. “The inflation technique completely solves the causal compatibility problem”. *Journal of Causal Inference* **8**, 70–91 (2020).
- [35] Sandu Popescu and Daniel Rohrlich. “Quantum nonlocality as an axiom”. *Foundations of Physics* **24**, 379–385 (1994).
- [36] Ivan Šupić, Jean-Daniel Bancal, and Nicolas Brunner. “Quantum Nonlocality in Networks Can Be Demonstrated with an Arbitrarily Small Level of Independence between the Sources”. *Physical Review Letters* **125**, 240403 (2020).
- [37] Rafael Chaves, George Moreno, Emanuele Polino, Davide Poderini, Iris Agresti, Alessia Suprano, Mariana R. Barros, Gonzalo Carva-

cho, Elie Wolfe, Askery Canabarro, Robert W. Spekkens, and Fabio Sciarrino. “Causal networks and freedom of choice in bell’s theorem”. [PRX Quantum](#) **2** (2021).